Journal of Marine Science and Technology (2023) 28:72–86
https://doi.org/10.1007/s00773-022-00904-7

ORIGINAL ARTICLE

Practical estimation method for extreme value distribution of von Mises stress in ship structure

Sadaoki Matsui[1]

Received: 5 January 2022 / Accepted: 30 August 2022 / Published online: 23 October 2022

Abstract

This study presents a practical method for estimating the extreme value distribution of von Mises stress for ship structural strength evaluations. The previous methods of calculating this distribution require somewhat complicated numerical calculations, such as multi-dimensional integration. In contrast, the proposed method is based on an asymptotic approximation and can be easily calculated in a similar way to the conventional linear statistical prediction. A closed expression was derived in the case of stress components which have non-zero mean value. The formula is derived under approximations that reflect realistic stress conditions when ships are under severe sea states. Through a structural analysis of a whole ship, it was comprehensively verified that the proposed method has sufficiently high accuracy for structural strength evaluation. Furthermore, a parametric analysis was conducted to clarify its limit of applicability.

Keywords Extreme value distribution · Von Mises stress · Non-Gaussian random process · Asymptotic approximation · Ship structural strength evaluation · Direct load and structure analysis

List of symbols

General

In the following, $\mathbf{G}(t) = \left\{G_1(t), G_2(t), G_3(t)\right\}^{\mathrm{T}}$ and $\mathbf{H}(t) = \left\{H_1(t), H_2(t), H_3(t)\right\}^{\mathrm{T}}$ are dummy variables that represent the vector process:

$\dot{\mathbf{G}}(t)$	Time derivative of $\mathbf{G}(t)$
$\mathbf{g}$	Realization of $\mathbf{G}(t)$
$\boldsymbol{\mu}_{\mathbf{G}}$	Mean value of $\mathbf{G}(t)$
$\boldsymbol{\sigma}_{\mathbf{G}}$	Standard deviation of $\mathbf{G}(t)$
$\boldsymbol{\Sigma}_{\mathbf{GH}}$	Covariance matrix between $\mathbf{G}(t)$ and $\mathbf{H}(t)$
$\rho_{G_iH_j}$	Correlation coefficients between $G_i(t)$ and $H_j(t)$
$f_{\mathbf{G}}(\mathbf{g})$	Joint probability density function between $G_1(t), G_2(t),$ and$G_3(t)$

Others

c_{ij}	Nondimensional coefficient related to the curvature of the isosurface of $f_{\mathbf{Y}}(\mathbf{y})$
g	Gravity acceleration
$Q_Z(z)$	Extreme value distribution (probability that the maxima of $Z(t)$ exceeds z)
T_{ze}	Encountered mean zero-upcrossing wave period
T_{zY_i}	Mean zero-upcrossing period of $Y_i(t) - \mu_{Y_i}$
U	Ship speed
$\nu_Z^+(z)$	Upcrossing rate at level $Z(t) = z$
$\mathbf{X}(t)$	Gaussian vector process of plane stress consisting of normal stress components (X_1, X_2) and share stress component (X_3)
$\hat{X}_i(\omega, \beta)$	Response amplitude operator of $X_i(t)$
$\mathbf{Y}(t)$	Gaussian vector process obtained by linear transformation of $\mathbf{X}(t)$
y_1^P, y_2^P	Coordinates of y_1 and y_2 on plane-P satisfying $y_3 = \mu_{Y_3}$
$y_1^M(z), y_2^M(z)$	Coordinates of y_1^P and y_2^P in which ψ takes maxima on the isoline $Z(t) = z$
$Z(t)$	Square of von Mises stress
Z_0	Value of $Z(t)$ in pre-load
z	Threshold of $Z(t)$
β	Wave angle (= 0: following sea, = π: head sea)
$\varepsilon_{X_i}(\omega, \beta)$	Phase advance of $\hat{X}_i(\omega, \beta)$
θ	Latitude in $\mathbf{y}$-space
$\Phi_{\zeta\zeta}(\omega, \beta)$	Wave spectrum
ϕ	Longitude in $\mathbf{y}$-space
$\psi\left(y_1^P, y_2^P\right)$	Exponent of $f_{\mathbf{Y}}(\mathbf{y})$ on plane-P

✉ Sadaoki Matsui
matsui-s@m.mpat.go.jp

[1] National Maritime Research Institute, 6-38-1, Shinkawa, Mitaka, Tokyo, Japan

ω	Wave frequency
ω_e	Encounter wave frequency

1 Introduction

A structural strength evaluation of a ship requires an estimate of the maximum response over the entire period of the ship's operation. The short/long-term prediction method based on linear theory proposed by Fukuda [1] is widely used for ship design because it can be easily calculated from the response amplitude operation (RAO) in the frequency domain and gives reasonable results. However, the method cannot deal with nonlinear quantities such as von Mises stress because it assumes that the response is linear and its extreme value distribution follows a Rayleigh distribution. Even though an estimation of the maximum expected value for von Mises stress is quite important for structural strength evaluations, there are still no methods that are widely adapted for ship structural design.

The estimation of the extreme value distribution of von Mises stress can be interpreted as an outcrossing problem on a hypersurface in stress component space, and it is defined by the integral of the probability density function on the hypersurface [2]. The integral cannot be solved analytically in the general case, and numerical approaches are needed to some extent. Although the methods presented in previous studies provide reasonable results [2–4], their computational procedures are somewhat complicated, e.g., involving a multi-dimensional numerical integration, and it seems difficult to apply them in practice. For a method to be practical, it must be not only accurate, but also computationally efficient and robust. These features are even more important for ship design because the contributions of all possible sea states must be taken into account when calculating the long-term probability of exceedance.

In terms of computational cost and robustness, the asymptotic approximation of the integral is a very effective approach. There have been several studies on asymptotic formulae of the extreme value distribution of non-Gaussian processes [5–7]. However, closed-form expressions for them are limited to special cases. Specifically, a formula for von Mises stress has not been presented for the case that the stress components have non-zero mean value, i.e., when stress in still-water conditions is considered. Since the still-water loads acting on a ship can be as significant as wave-induced loads, it is essential to consider the mean value of stress components in a structural strength evaluation of a ship.

In light of the above background, the purpose of this paper is to develop a practical method for calculating the extreme value distribution of von Mises stress that is accurate, computationally efficient, and robust. The method assumes that there are three stress components (plane stress conditions) which follow a narrow-band stationary Gaussian process. Here, the author has developed a closed formula for the extreme value distribution that is based on an asymptotic expansion of the integral by an extension of Laplace's method. In particular, the proposed formula takes into account the non-zero mean values in closed form, which has not been shown in previous studies [5–7]. In deriving the formula, approximations are applied to the extent that accuracy does not deteriorate under realistic stress conditions in which the ship is under severe sea states. The applicability of proposed method is verified comprehensively by conducting a whole ship structural analysis in waves.

2 Formulation of extreme value distribution of von Mises stress

First, we define the random process of stress components and von Mises stress. Next, for the sake of simplicity, we introduce a variable transformation of the stress components and express von Mises stress in a sum-of-squares form. Then, we define the extreme value distribution in terms of the upcrossing rate and finally give a specific formulation of the extreme value distribution of von Mises stress using stochastic parameters of the stress components.

2.1 Definition of a random process

Let $X_1(t)$ and $X_2(t)$ be normal stress components and $X_3(t)$ be the shear stress component of the plane stress at a certain position in a ship structure. Furthermore, let us assume them to be random variables following a stationary Gaussian distribution in short-term sea states. Their mean values $\mu_{X_i}\left(:=E\left[X_i(t)\right]\right)$ are interpreted as the stress occurring in the still-water condition. Voigt's notation for them, $\mathbf{X}(t)\left(:=\left\{X_1(t),X_2(t),X_3(t)\right\}^{\mathrm{T}}\right)$, is a Gaussian vector process with mean value vector $\boldsymbol{\mu}_{\mathbf{X}}\left(:=\left\{\mu_{X_1},\mu_{X_2},\mu_{X_3}\right\}^{\mathrm{T}}\right)$ and covariance matrix $\boldsymbol{\Sigma}_{\mathbf{XX}}\left(\Sigma_{XiXj}:=E\left[\left(X_i(t)-\mu_{Xi}\right)-\left(X_j(t)-\mu_{Xj}\right)\right]\right)$. The joint probability density function (PDF) of $\mathbf{X}(t)$ is

$$f_{\mathbf{X}}(\mathbf{x})=\frac{1}{\sqrt{(2\pi)^3\det\left|\boldsymbol{\Sigma}_{\mathbf{XX}}\right|}}\times\exp\left[-\frac{1}{2}\left(\mathbf{x}-\boldsymbol{\mu}_{\mathbf{X}}\right)^{\mathrm{T}}\boldsymbol{\Sigma}_{\mathbf{XX}}^{-1}\left(\mathbf{x}-\boldsymbol{\mu}_{\mathbf{X}}\right)\right]. \tag{1}$$

The state is also denoted as $\mathbf{X}(t)\sim\mathcal{N}\left(\boldsymbol{\mu}_{\mathbf{X}},\boldsymbol{\Sigma}_{\mathbf{XX}}\right)$. The time derivative of $\mathbf{X}(t)$, denoted as $\dot{\mathbf{X}}(t)$, is a stationary Gaussian vector process with zero mean, i.e., $\dot{\mathbf{X}}(t)\sim\mathcal{N}\left(0,\boldsymbol{\Sigma}_{\dot{\mathbf{X}}\dot{\mathbf{X}}}\right)$. In addition, the covariance matrix between $\mathbf{X}(t)$ and $\dot{\mathbf{X}}(t)$ is

$\Sigma_{\mathbf{X}\dot{\mathbf{X}}}\left(=\Sigma_{\dot{\mathbf{X}}\mathbf{X}}^{\mathrm{T}}, \Sigma_{X_i\dot{X}_j} \coloneqq E\left[\left(X_i(t)-\mu_{X_i}\right)\dot{X}_j(t)\right]\right)$. Since the Gaussian process $X_i(t)$ and its time derivative $\dot{X}_i(t)$ are mutually independent, the diagonal components of $\mathbf{\Sigma}_{\mathbf{X}\dot{\mathbf{X}}}$ are all zero.

The square of the von Mises stress $Z(t)$ is expressed in the following quadratic form of the stress components.

$$Z(t) = \mathbf{X}(t)^{\mathrm{T}}\mathbf{A}\mathbf{X}(t), \tag{2}$$

$$\text{where } \mathbf{A} = \begin{bmatrix} 1 & -1/2 & 0 \\ -1/2 & 1 & 0 \\ 0 & 0 & 3 \end{bmatrix}. \tag{3}$$

The symbol for the time variable (t) of the random process is omitted hereafter.

2.2 Variable transformation

To simplify the extreme value distribution of Z in Eq. (2), we will transform the stress component vector $\mathbf{X}$ into another Gaussian vector process $\mathbf{Y}$ such that Z can be expressed in sum-of-squares form, according to the procedure presented by Segalman [8, 9].

$$Z = \sum_{i=1}^{3} Y_i^2. \tag{4}$$

The vector process $\mathbf{Y}$ follows $\mathbf{Y} \sim \mathcal{N}\left(\boldsymbol{\mu}_{\mathbf{Y}}, \mathbf{\Sigma}_{\mathbf{YY}}\right)$, where $\mathbf{\Sigma}_{\mathbf{YY}}$ is the following diagonal matrix:

$$\mathbf{\Sigma}_{\mathbf{YY}} = \mathrm{diag}\left(\sigma_{Y_1}^2, \sigma_{Y_2}^2, \sigma_{Y_3}^2\right). \tag{5}$$

The variable transformation $\mathbf{X} \rightarrow \mathbf{Y}$ can be applied when Z is a quadratic form of $\mathbf{X}$. Appendix 1 shows the procedure of the transformation, which is a modification of Segalman's in which only one diagonalization is required. Furthermore, Appendix 1 shows how to obtain the covariance matrixes $\mathbf{\Sigma}_{\mathbf{XX}}$, $\mathbf{\Sigma}_{\mathbf{X}\dot{\mathbf{X}}}$, and $\mathbf{\Sigma}_{\dot{\mathbf{X}}\mathbf{X}}$ from the RAOs of the stress components for the case of a ship has advancing speed in short-crested irregular waves.

The mean value of Z can be expressed as follows.

$$\mu_Z = Z_0 + \sum_{i=1}^{3} \sigma_{Y_i}^2, \tag{6}$$

where

$$Z_0 \coloneqq \sum_{i=1}^{3} \mu_{Y_i}^2 = \boldsymbol{\mu}_{\mathbf{X}}^{\mathrm{T}}\mathbf{A}\boldsymbol{\mu}_{\mathbf{X}}, \tag{7}$$

Z_0 means the value of Z in pre-load, i.e., in still-water condition.

2.3 Definition of extreme value distribution

As it is well known, the number of maxima can be approximated by the number of upcrossings for a narrow-band process whose minima are not so high in value. Therefore, the extreme value distribution $Q_Z(z)$, i.e., the probability that an extreme value exceeds $Z = z$, can be approximated as follows.

$$Q_Z(z) \cong \frac{\left(\begin{array}{c}\text{Number of upcrossings at} Z = z \\ \text{per unit time}\end{array}\right)}{\left(\text{Number of maxima per unit time}\right)} = T_p \nu_Z^+(z), \tag{8}$$

where T_p is the mean period between maxima of Z, and $\nu_Z^+(z)$ is the upcrossing rate at level z. The definition of (2.8), however, is not suitable for a statistical prediction of von Mises stress, because it is difficult to formulate T_p. In addition, the number of maxima of von Mises stress is about twice that of the maxima of the stress component; hence, definition by Eq. (8) is a different index from the exceedance probability of the conventional short/long-term prediction method.

Instead, the following definition is used in this study.

$$Q_Z(z) \coloneqq T_{ze}\nu_Z^+(z), \tag{9}$$

where T_{ze} is the encountered mean zero-upcrossing wave period, which considers the effect of the ship advancing into waves,

$$T_{ze} \coloneqq 2\pi\sqrt{\frac{\int_{-\pi}^{\pi}\int_0^{\infty}\Phi_{\zeta\zeta}(\omega,\beta)\mathrm{d}\omega\mathrm{d}\beta}{\int_{-\pi}^{\pi}\int_0^{\infty}\omega_e^2\Phi_{\zeta\zeta}(\omega,\beta)\mathrm{d}\omega\mathrm{d}\beta}}, \tag{10}$$

where

$$\omega_e = \omega - \frac{U}{g}\omega^2\cos\beta, \tag{11}$$

is the encounter wave frequency and $\Phi_{\zeta\zeta}$, ω, β, U, and g are the wave spectrum, wave frequency, wave angle, ship speed, and gravity acceleration, respectively. T_{ze} is approximately equal to the mean zero-upcrossing period of the fluctuation components of stress $X_i - \mu_{X_i}$.

As defined in Eq. (9), the maximum expected value of Z occurring once in N-waves coincides with z satisfying $Q_Z(z) = 1/N$ and can be treated in the same way as the index of the exceedance probability used in the conventional short/long-term prediction method. Strictly speaking, it is not accurate to call it an exceedance probability because Eq. (9) is an expected value of upcrossings in terms of T_{ze} and can exceed 1. However, for the purpose of estimating the maximum expected value of Z in a certain duration, which is used for short/long-term prediction, definition by Eq. (9) is appropriate and the fact that $Q_z(z)$ exceeds 1 does not cause any problems.

2.4 Formulation of the upcrossing rate

Upcrossing rate $v_Z^+(z)$ can be calculated using Rice's formula [10]:

$$v_Z^+(z) = \int_0^\infty \dot{z} f_{Z\dot{Z}}(z, \dot{z}) \mathrm{d}\dot{z}, \tag{12}$$

where $f_{Z\dot{Z}}(z, \dot{z})$ is the joint PDF of Z and its time derivative $\dot{Z}$. Gupta proposed a direct way to find $f_{Z\dot{Z}}(z, \dot{z})$ for von Mises stress [4].

Veneziano generalized Rice's formula (12) and presented the following equation for the case, where Z is expressed as a general scalar function of X_i [2].

$$v_Z^+(z) = \int_{\partial B(z)} f_{\mathbf{X}}(\mathbf{x}) \int_0^\infty \dot{x}_n f_{\dot{X}_n|\mathbf{X}=\mathbf{x}}\left(\dot{x}_n|\mathbf{x}\right) \mathrm{d}\dot{x}_n \mathrm{d}\partial B, \tag{13}$$

where $\partial B(z)$ is an isosurface of $Z = z$ in $\mathbf{x}$-space, $\dot{X}_n$ is the component of $\dot{\mathbf{X}}$ at a point $\mathbf{x} \in \partial B(z)$ in the direction normal to the ellipsoid and directed outward, and $f_{\dot{X}_n|\mathbf{X}=\mathbf{x}}\left(\dot{x}_n|\mathbf{x}\right)$ is the conditional PDF of $\dot{X}_n$.

Madsen derived a specific form for Eq. (13) in the case that Z is the square of von Mises stress and $\mathbf{X}$ consists of three stress components [3]. For Madsen's expression, using the variable $\mathbf{Y}$ in Eq. (4) instead of $\mathbf{X}$, the upcrossing rate can be expressed as

$$\begin{aligned} v_Z^+(z) = z \int_0^\pi \mathrm{d}\theta \sin\theta \int_0^{2\pi} \mathrm{d}\phi f_{\mathbf{Y}}(\mathbf{y}) \\ \times \left[\frac{\mu_{\dot{Y}_n}}{2} \left\{ 1 + \mathrm{erf}\left[\frac{\mu_{\dot{Y}_n}}{\sqrt{2}\sigma_{\dot{Y}_n}} \right] \right\} \right. \\ \left. + \frac{\sigma_{\dot{Y}_n}}{\sqrt{2\pi}} \exp\left[-\frac{1}{2} \left(\frac{\mu_{\dot{Y}_n}}{\sigma_{\dot{Y}_n}} \right)^2 \right] \right], \end{aligned} \tag{14}$$

where

$$f_{\mathbf{Y}}(\mathbf{y}) = \prod_{i=1}^{3} \frac{1}{\sqrt{2\pi}\sigma_{Y_i}} \exp\left[-\frac{\left(y_i - \mu_{Y_i}\right)^2}{2\sigma_{Y_i}^2} \right], \tag{15}$$

$$\mathbf{y} = \begin{Bmatrix} \sqrt{z}\sin\theta\cos\phi \\ \sqrt{z}\sin\theta\sin\phi \\ \sqrt{z}\cos\theta \end{Bmatrix}, \tag{16}$$

$$\mu_{\dot{Y}_n} = \mathbf{n}^{\mathrm{T}} \boldsymbol{\Sigma}_{\dot{\mathbf{Y}}\mathbf{Y}} \boldsymbol{\Sigma}_{\mathbf{Y}\mathbf{Y}}^{-1} \left(\mathbf{y} - \boldsymbol{\mu}_{\mathbf{Y}} \right), \tag{17}$$

$$\sigma_{\dot{Y}_n}^2 = \mathbf{n}^{\mathrm{T}} \left(\boldsymbol{\Sigma}_{\dot{\mathbf{Y}}\dot{\mathbf{Y}}} - \boldsymbol{\Sigma}_{\dot{\mathbf{Y}}\mathbf{Y}} \boldsymbol{\Sigma}_{\mathbf{Y}\mathbf{Y}}^{-1} \boldsymbol{\Sigma}_{\mathbf{Y}\dot{\mathbf{Y}}} \right) \mathbf{n}, \tag{18}$$

$$\mathbf{n} = \begin{Bmatrix} \sin\theta\cos\phi \\ \sin\theta\sin\phi \\ \cos\theta \end{Bmatrix}. \tag{19}$$

Although it is an exact formula without any special assumptions, this formula is not so practical because it requires a numerical solution of the double integral. Moreover, it is difficult to ensure its reliability for cases where the matrix $\boldsymbol{\Sigma}_{\mathbf{YY}}$ $(= \mathrm{diag}(\sigma_{Y_1}^2, \sigma_{Y_2}^2, \sigma_{Y_3}^2))$ is close to being singular, as is often the case.

3 Asymptotic formula of the upcrossing rate

This section derives a practical closed formula for the upcrossing rate $v_Z^+(z)$ by adapting an asymptotic expansion and making some approximations of the integral in Eq. (14).

3.1 Formulation assuming that components are mutually independent

Let us assume that $\mathbf{Y}$ and their time derivatives $\dot{\mathbf{Y}}$ are mutually independent. In this case,

$$\boldsymbol{\Sigma}_{\dot{\mathbf{Y}}\mathbf{Y}} \cong 0, \boldsymbol{\Sigma}_{\mathbf{Y}\dot{\mathbf{Y}}} \cong 0, \tag{20}$$

$$\boldsymbol{\Sigma}_{\dot{\mathbf{Y}}\dot{\mathbf{Y}}} \cong \mathrm{diag}\left(\sigma_{\dot{Y}_1}^2, \sigma_{\dot{Y}_2}^2, \sigma_{\dot{Y}_3}^2 \right), \tag{21}$$

and Eq. (14) can be simplified as

$$v_Z^+(z) \cong \frac{z}{\sqrt{2\pi}} \int_0^\pi \mathrm{d}\theta \sin\theta \int_0^{2\pi} \mathrm{d}\phi \sigma_{\dot{Y}_n} f_{\mathbf{Y}}(\mathbf{y}), \tag{22}$$

where

$$\begin{aligned} \sigma_{\dot{Y}_n}^2 &\cong \mathbf{n}^{\mathrm{T}} \boldsymbol{\Sigma}_{\dot{\mathbf{Y}}\dot{\mathbf{Y}}} \mathbf{n} \\ &\cong \sigma_{\dot{Y}_1}^2 \sin^2\theta\cos^2\phi + \sigma_{\dot{Y}_2}^2 \sin^2\theta\sin^2\phi + \sigma_{\dot{Y}_3}^2 \cos^2\theta. \end{aligned} \tag{23}$$

It can be confirmed that the same result is derived by Fukuda's derivation procedure [11], which makes the same approximations as in Eqs. (20) and (21). It has been theoretically shown by Hagen that the effect of the approximation in Eq. (20) on $v_Z^+(z)$ is secondary, and the loss of accuracy can be ignored [6]. On the other hand, Eq. (21) is not general and does not hold in all cases. However, as we will see in Sect. 4, Eq. (21) holds in most cases without any problem, because when $\mathbf{X}$ is orthogonally transformed, the covariance matrix $\boldsymbol{\Sigma}_{\dot{\mathbf{Y}}\dot{\mathbf{Y}}}$ is almost diagonalized.

When $\sigma_{Y_2}/\sigma_{Y_1}$ and $\sigma_{Y_3}/\sigma_{Y_1}$ are close to zero, the exponential part of Eq. (22) changes sharply, making it difficult to ensure the accuracy of the numerical integration. In particular, $\sigma_{Y_3}/\sigma_{Y_1}$ often takes a very small value. Consequently, we next derive the asymptotic formulae of Eq. (22) for the case where $\sigma_{Y_3}/\sigma_{Y_1}$ are close to zero.

When $\sigma_{Y_3}/\sigma_{Y_1} \to 0$, the integral on the right-hand side of Eq. (22) is dominated by the contribution of the integrand from the vicinity of the plane-P formed by $y_3 = \mu_{Y_3}$. In this case, except for the exponential function of y_3, the change with respect to y_3 is gradual, so it can be represented by the value on the plane-P. Hence, the following asymptotic approximation is derived by applying the Gaussian integral formula.

$$\sqrt{z}\int_0^{\pi} \mathrm{d}\theta \sin\theta \exp\left[-\frac{\left(y_3-\mu_{Y_3}\right)^2}{2\sigma_{Y_3}^2}\right] \sim \sqrt{2\pi}\sigma_{Y_3} \tag{24}$$

as $\sigma_{Y_3}/\sigma_{Y_1} \to 0$.

Accordingly, the upcrossing rate asymptotically follows as

$$v_Z^+(z) \sim \frac{\zeta}{(2\pi)^{3/2}\sigma_{Y_1}\sigma_{Y_2}} \int_0^{2\pi} \sigma_{\dot{Y}_n}^P \exp[\psi]\mathrm{d}\phi \tag{25}$$

as $\sigma_{Y_3}/\sigma_{Y_1} \to 0$,

where

$$\sigma_{\dot{Y}_n}^P := \sqrt{\sigma_{\dot{Y}_1}^2\cos^2\phi + \sigma_{\dot{Y}_2}^2\sin^2\phi}, \tag{26}$$

$$\psi\left(y_1^P, y_2^P\right) := -\frac{\left(y_1^P-\mu_{Y_1}\right)^2}{2\sigma_{Y_1}^2} - \frac{\left(y_2^P-\mu_{Y_2}\right)^2}{2\sigma_{Y_2}^2}, \tag{27}$$

$$\begin{cases} y_1^P(z,\phi) = \zeta\cos\phi \\ y_2^P(z,\phi) = \zeta\sin\phi \end{cases}, \tag{28}$$

$$\zeta := \sqrt{z-\mu_{Y_3}^2}. \tag{29}$$

y_1^P and y_2^P are the coordinates of y_1 and y_2 on plane-P, as shown in Fig. 1. In this case, $v_Z^+(z) = 0$ when $z \le \mu_{Y_3}^2$ because Z cannot be less than $\mu_{Y_3}^2$.

In addition to $\sigma_{Y_3}/\sigma_{Y_1} \to 0$, if $\sigma_{Y_2}/\sigma_{Y_1} \to 0$, the following equation can be derived because the integral of Eq. (25) is dominated by the contribution of the integrand in the vicinity of line-L formed by $\left(y_2, y_3\right) = \left(\mu_{Y_2}, \mu_{Y_3}\right)$.

$$v_Z^+(z) \sim \frac{2}{T_{zY_1}} \exp\left[-\frac{(y_1^L)^2+\mu_{Y_1}^2}{2\sigma_{Y_1}^2}\right] \cosh\left(\frac{y_1^L\mu_{Y_1}}{\sigma_{Y_1}^2}\right) \tag{30}$$

as $\sigma_{Y_2}/\sigma_{Y_1} \to 0$ and $\sigma_{Y_3}/\sigma_{Y_1} \to 0$,

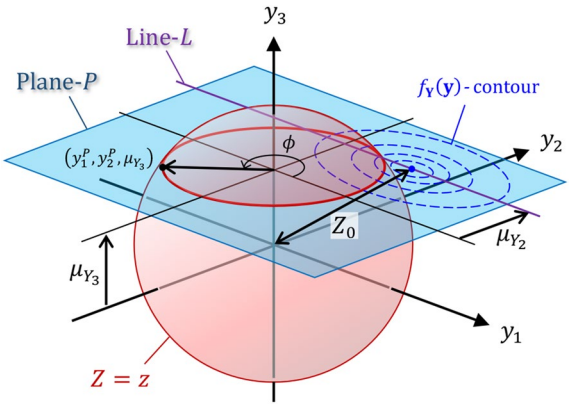

Fig. 1 Schema of plane-P and line-L in $\mathbf{y}$-space

where $y_1^L(z) := \sqrt{z-\mu_{Y_2}^2-\mu_{Y_3}^2}$ (31)

and $T_{zY_1}\left(:= 2\pi\sigma_{Y_1}/\sigma_{\dot{Y}_1}\right)$ is the mean zero-upcrossing period of $Y_1 - \mu_{Y_1}$. In this case, $v_Z^+(z) = 0$ when $z \le \mu_{Y_2}^2 + \mu_{Y_3}^2$. Expression of Eq. (30) is simple and is suitable for a rough order evaluation of z. When we set $Q_Z(z) \cong T_{zY_1}v_Z^+(z)$ and solve for z, we get

$$z(Q_Z) \cong \left\{\sigma_{Y_1}\sqrt{-2\ln\left(Q_Z\right)} + \mu_{Y_1}\right\}^2 + \mu_{Y_2}^2 + \mu_{Y_3}^2. \tag{32}$$

This formula is not accurate, but it is useful as a reference value for calculating the distribution of $Q_Z(z)$ while varying z.

3.2 Asymptotic expansion of Eq. (25)

Here, we derive a more practical formula without an integral or case separation on the basis of an asymptotic expansion using Laplace's method.

Even though the Laplace's method is a series representation of the Laplace integral under the assumption that z is sufficiently large, it is known to be a good approximation over a wide range even if only the first term is considered [14]. When $\boldsymbol{\mu}_{\mathbf{Y}} = 0$, the integral in Eq. (22) becomes the Laplace integral, so we can directly apply Laplace's method. Appendix 2 derives the following asymptotic formula:

$$v_Z^+(z) \sim \frac{2}{T_{zY_1}}\sqrt{c_{21}c_{31}} \exp\left[-\frac{z}{2\sigma_{Y_1}^2}\right] \tag{33}$$

when $\boldsymbol{\mu}_{\mathbf{Y}} = 0$, as $z \to \infty$,

where

$$c_{ij} \coloneqq \frac{1}{1-\left(\sigma_{Y_i}^2/\sigma_{Y_j}^2\right)} \tag{34}$$

is a nondimensional coefficient related to the curvature of the isosurface of $f_{\mathbf{Y}}(\mathbf{y})$ on y_iy_j-plane. Equation (33) coincides with Breitung's result [5].

On the other hand, the derivation is not straightforward when $\boldsymbol{\mu}_{\mathbf{Y}} \neq 0$, because it is difficult to explicitly express the coordinates of the reference points for the Taylor expansion. In this study, the coordinates of the reference points are approximated. Equation (25) is used as the base formula of the asymptotic expansion, because $\sigma_{Y_3}/\sigma_{Y_1}$ usually does not take a large value, as will be shown in Sect. 4.

In taking the asymptotic expansion of Eq. (25), we must find the angle ϕ^M where ψ is maximized on the isosurface of Z (the circle formed by the intersection of the plane-P and the isosurface of Z) and consider the contribution of the integrand only in the vicinity of ϕ^M. In the case of the integral in Eq. (25), there are usually two maxima of ψ and the contribution of the second largest maximum cannot be ignored in the case $\mu_{Y_1} \ll \sigma_{Y_1}$. Therefore, to consider both two maxima, let us denote the (y_1^P, y_2^P)-coordinates where ψ is at a maximum by $\left(y_1^{M+}, y_2^{M+}\right)$ and $\left(y_1^{M-}, y_2^{M-}\right)$. The sign of $M\pm$ corresponds to the sign of y_1^P.

According to Laplace's method, Eq. (25) is expanded as follows (see Appendix 2):

$$v_Z^+(z) \sim \frac{\sqrt{c_{31}}}{2\pi\sigma_{Y_1}\sigma_{Y_2}}\left\{\left.\frac{\zeta\sigma_{\dot{Y}_n}^P \exp[\psi]}{\sqrt{-\psi_{\phi\phi}}}\right|_{(y_1^P,y_2^P)=(y_1^{M+},y_2^{M+})} + \left.\frac{\zeta\sigma_{\dot{Y}_n}^P \exp[\psi]}{\sqrt{-\psi_{\phi\phi}}}\right|_{(y_1^P,y_2^P)=(y_1^{M-},y_2^{M-})}\right\} \tag{35}$$

as $z \to \infty$,

where

$$\psi_{\phi\phi}\left(y_1^{M\pm}, y_2^{M\pm}\right) = \left(\frac{1}{\sigma_{Y_2}^2} - \frac{1}{\sigma_{Y_1}^2}\right) \times\left\{\left(y_2^{M\pm}\right)^2 - c_{21}\mu_{Y_2}y_2^{M\pm} - \left(y_1^{M\pm}\right)^2 + c_{12}\mu_{Y_1}y_1^{M\pm}\right\}, \tag{36}$$

$$\zeta\sigma_{\dot{Y}_n}^P\left(y_1^{M\pm}, y_2^{M\pm}\right) = \sqrt{\sigma_{\dot{Y}_1}^2\left(y_1^{M\pm}\right)^2 + \sigma_{\dot{Y}_2}^2\left(y_2^{M\pm}\right)^2}. \tag{37}$$

The coefficient $\sqrt{c_{31}}$ is additionally taken into account to consider the effect of $\sigma_{Y_3}/\sigma_{Y_1}$ by referring to the asymptotic formula (33)with zero mean.

Next, we find the points $(y_1^{M\pm}, y_2^{M\pm})$ where ψ reaches maximal value. They are at the intersections of the isoline of z

$$\left(y_1^P\right)^2 + \left(y_2^P\right)^2 = \zeta^2 \tag{38}$$

and the curve on which gradient of $\psi(y_1^P, y_2^P)$ is directed to the origin of the plane-P, that is,

$$\begin{Bmatrix}\partial\psi/\partial y_1^P\\ \partial\psi/\partial y_2^P\\ 0\end{Bmatrix} \times \begin{Bmatrix}y_1^P\\ y_2^P\\ 0\end{Bmatrix} = 0, \tag{39}$$

$$\leftrightarrow \left(y_1^P - c_{12}\mu_{Y_1}\right)\left(y_2^P - c_{21}\mu_{Y_2}\right) = c_{12}\mu_{Y_1}c_{21}\mu_{Y_2}. \tag{40}$$

Equation (40) is the hyperbola that passes through the origin $\left(y_1^P, y_2^P\right) = (0,0)$ as well as the mean value point $\left(y_1^P, y_2^P\right) = (\mu_{Y_2}, \mu_{Y_3})$ and is asymptotic to the two lines: $y_1^P = c_{12}\mu_{Y_1}$, and $y_2^P = c_{21}\mu_{Y_2}$. The schema of the contour of z and ψ on plane-P and hyperbola of Eq. (40) which ψ takes an extreme value is shown in Fig. 2. From Fig. 2, it can be understood that ψ has two maxima and two minima on the contour line of Z and the maximum is in the region of $\text{sign}(\mu_{Y_1})\, y_1^P \geq 0$.

To obtain an explicit expression for $(y_1^{M\pm}, y_2^{M\pm})$, which is defined as the points that satisfy Eqs. (38) and (40) simultaneously, it is necessary to solve a quartic function and the closed formula of $(y_1^{M\pm}, y_2^{M\pm})$ becomes quite complicated. Therefore, we will treat this problem approximately. First, for simplicity, let us approximate the hyperbola of Eq. (40) as a symmetric curve which mirrors the hyperbola on the side of $\text{sign}(\mu_{Y_1})\, y_1^P \geq 0$ with respect to the y_2^P-axis, i.e., $y_2^{M+} = y_2^{M-} = y_2^M$. Then, as an explicit function of z, y_2^M can be approximated as follows:

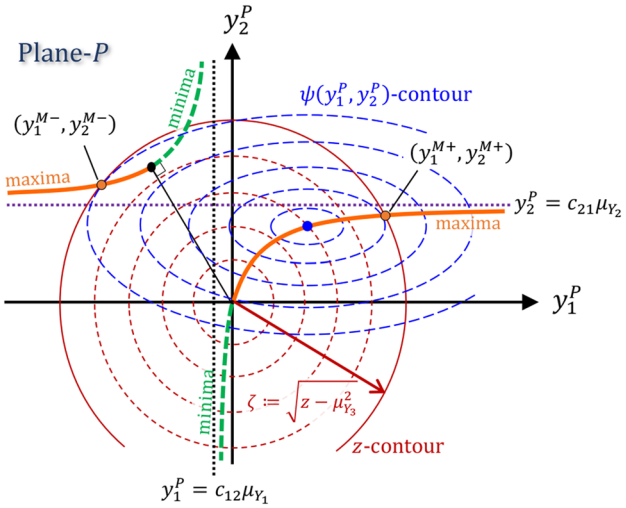

Fig. 2 Schema of maxima and minima of ψ on z-contour on the plane-P

$$y_2^M(z) \cong \frac{\mu_{Y_2}}{2\alpha}\left\{\zeta - c_{12}\left|\mu_{Y_1}\right| + \alpha c_{21} - \sqrt{\left(\zeta - c_{12}\left|\mu_{Y_1}\right| + \alpha c_{21}\right)^2 - 4\alpha c_{21}\zeta}\right\}, \tag{41}$$

where $\alpha := \sqrt{\mu_{Y_1}^2 + \mu_{Y_2}^2} - \left|\mu_{Y_1}\right|$. (42)

This formula has the following value when $\mu_{Y_1} = 0$, as can be seen by taking the limit $\mu_{Y_1} \to 0$.

$$y_2^M(z) = \min\left(c_{21}\mu_{Y_2}, \zeta\right) \text{ when } \mu_{Y_1} = 0. \tag{43}$$

The derivation of Eq. (41) is shown in Appendix 3. The approximation formula (41) is a curve whose asymptotic behavior as $z \to \infty$ is correct on the order of $O(1/\zeta)$ compared to the true solution, and the curve passes through the origin and the mean value point (μ_{Y_1}, μ_{Y_2}) at $z = 0$ and $z = Z_0$, respectively. Furthermore, it always satisfies $y_2^M < \zeta$ when $z \geq Z_0$ so that the square root of y_1^M does not become negative. Once y_2^M is obtained, $y_1^{M\pm}$ is determined from Eq. (38) to be

$$y_1^{M\pm} = \pm y_1^M = \pm\sqrt{\zeta^2 - \left(y_2^M\right)^2}. \tag{44}$$

After substituting the above formulae for $\left(\pm y_1^M, y_2^M\right)$ into Eqs. (35)–(37), the following approximation for the coefficient part $(\zeta\sigma_{\dot{Y}_n}^P / \sqrt{-\psi_{\phi\phi}})$ is applied.

$$\sqrt{\frac{\sigma_{\dot{Y}_1}^2\left(y_1^M\right)^2 + \sigma_{\dot{Y}_2}^2\left(y_2^M\right)^2}{\left(y_1^M\right)^2 \mp c_{12}\mu_{Y_1}y_1^M - \left(y_2^M\right)^2 + c_{21}\mu_{Y_2}y_2^M}} \cong \sigma_{\dot{Y}_1}\sqrt{\frac{1}{1 - \frac{c_{12}\left|\mu_{Y_1}\right|}{y_1^M}}}. \tag{45}$$

This approximation is valid because the coefficient part has less impact than the exponential part $\exp[\psi]$ and is meaningful in the sense of avoiding a singularity ($1 - c_{12}\left|\mu_{Y_1}\right|/y_1^M$ always takes positive value). Accordingly, the upcrossing rate in Eq. (35) can be rewritten as follows.

$$v_Z^+(z) \cong \frac{1}{T_{zY_1}}\sqrt{\frac{c_{21}c_{31}}{1 - \frac{c_{12}\left|\mu_{Y_1}\right|}{y_1^M}}}\exp\left[-\frac{\left(y_2^M - \mu_{Y_2}\right)^2}{2\sigma_{Y_2}^2}\right] \times\left\{\exp\left[-\frac{\left(y_1^M + \mu_{Y_1}\right)^2}{2\sigma_{Y_1}^2}\right] + \exp\left[-\frac{\left(y_1^M - \mu_{Y_1}\right)^2}{2\sigma_{Y_1}^2}\right]\right\}. \tag{46}$$

(Proposed)

This is a practical formula that does not require numerical integration and is valid in the region $z \geq Z_0$. Equation (46) coincides with Eq. (33) when $\mu_{Y_i} = 0$. To calculate the extreme value distribution $Q_Z(z)$, Eq. (46) requires only σ_{Y_i} and μ_{Y_i} when $Q_Z(z) \cong T_{zY_1}v_Z^+(z)$ holds (in Sect. 4 indicates that this approximation is usually valid).

4 Numerical validations

4.1 Target ship structural model for analysis

To validate the applicability of the proposed extreme value distribution formula (46) to ship structural design, a direct load and structure analysis of a whole ship FEM model was conducted using the DLSA-Basic system [15], wherein wave-induced stresses and still-water stresses were obtained of all shell elements. The target model was a bulk carrier with $L = 280$m, and the full load condition with homogeneous loading (homo.) and alternative loading (alt.) were considered. For each condition, conventional short/long-term predictions were performed for the three stress components in the neutral plane of all shell elements, and the top 100 elements of the long-term maximum expected value (including the still-water component) were selected for each seven-element group where the mean wave angle in the MSS (Most Severe Short-term sea states) [16] was 0°, 30°, …, 180°. The selected 700 elements can be regarded as the primary structural members affected by various load factors in all wave directions and are considered suitable for comprehensive verification. Figure 3 shows the ship FEM model with the selected elements highlighted in the homo./alt. conditions.

4.2 Histogram of stochastic parameters of selected elements in the most severe short-term sea state

Before the numerical validation, in order to capture a realistic range of stochastic parameters of the stress vector process,

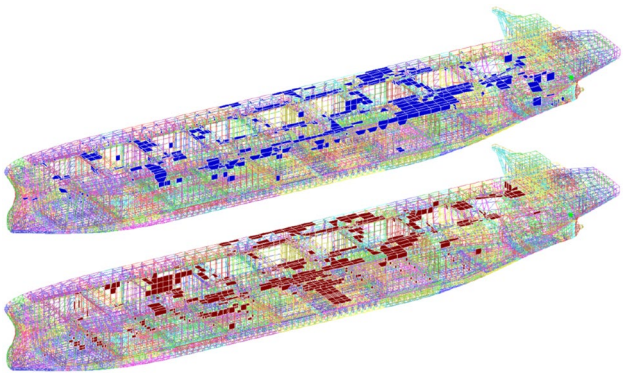

Fig. 3 700 elements selected for numerical validation (above: homo., below: alt.)

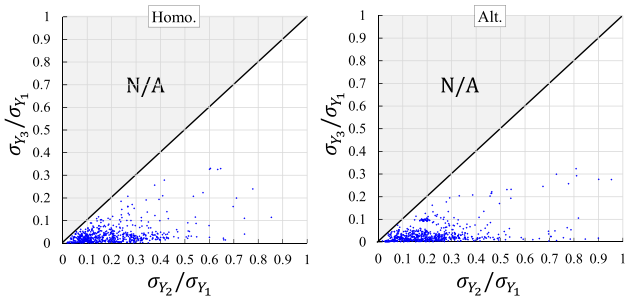

Fig. 4 Scatter plots on plane of the standard deviation ratio $\sigma_{Y_2}/\sigma_{Y_1}$ and $\sigma_{Y_3}/\sigma_{Y_1}$ for the 700 selected elements (left: homo., right: alt.)

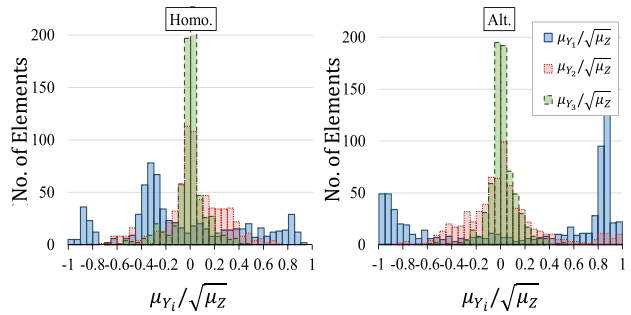

Fig. 5 Histograms of mean values μ_{Y_i} normalized by square root of μ_Z $(= \sum_{i=1}^{3}(\mu_{Y_i}^2 + \sigma_{Y_i}^2))$ for the 700 selected elements (left: homo., right: alt.)

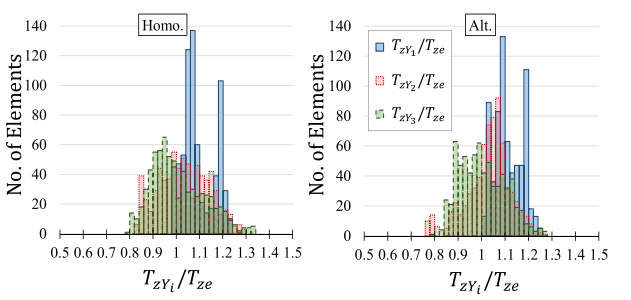

Fig. 6 Histograms of ratios of mean zero-upcrossing period of Y_i and incident wave for the 700 selected elements (left: homo., right: alt.)

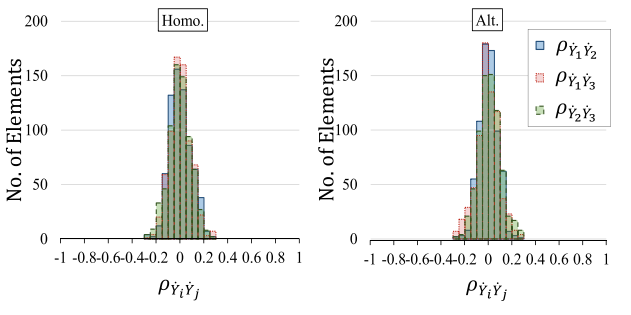

Fig. 7 Histograms of correlation coefficients of $\dot{Y}_i$ for the 700 selected elements (left: homo., right: alt.)

the mean value $\boldsymbol{\mu}_{\mathbf{Y}}$ and covariance matrixes $\boldsymbol{\Sigma}_{\mathbf{YY}}, \boldsymbol{\Sigma}_{\mathbf{Y\dot{Y}}}, \boldsymbol{\Sigma}_{\mathbf{\dot{Y}\dot{Y}}}$ of the vector process $\mathbf{Y}$ in the MSS, which is converted from the stress component vector $\mathbf{X}$ as presented in Appendix 1, were calculated for each of the 2 loading conditions × 700 elements.

Figure 4 shows scatter plots on the $\sigma_{Y_2}/\sigma_{Y_1}$-$\sigma_{Y_3}/\sigma_{Y_1}$ plane of 700 elements × 2 conditions. From the figure, almost all values of $\sigma_{Y_2}/\sigma_{Y_1}$ are less than 0.5 and almost all values of $\sigma_{Y_3}/\sigma_{Y_1}$ are less than 0.1 (maximum 0.33). When the standard deviation ratio $\sigma_{Y_2}/\sigma_{Y_1}$ is close to 1, the element is affected by two or more uncorrelated and comparable dominant load factors, e.g., vertical bending moment and roll motion under the MSS. The fact that $\sigma_{Y_3}/\sigma_{Y_1}$ is generally very small implies that the hull structural members are dominated by only two uncorrelated (and comparable) load factors. This fact might also hold in the case of a 3-dimensional stress condition. That is, when the six standard deviations $\sigma_{Y_1}, \ldots, \sigma_{Y_6}$ are obtained from the orthogonal transformation of six stress components of solid element and arranged in descending order, $\sigma_{Y_i}/\sigma_{Y_1}$ $(i \geq 3)$ might be negligible. Hence, we infer that the proposed formula (46), in which ζ is defined as $\zeta := \sqrt{(z - \sum_{i=3}^{6} \mu_{Y_i}^2)}$, is also applicable to a solid element.

Figure 5 shows histograms of ratios of the mean value of Y_i against the square root of the mean value of Z. Since the mean value of Z is $\mu_Z = \sum_{i=1}^{3}(\mu_{Y_i}^2 + \sigma_{Y_i}^2)$, as written in Eq. (6), the fact that the ratio is close to ±1 means that the mean value μ_{Y_i} is very large compared to the wave-induced component. Figure 5 confirms that their ratios are in wide range and are close to ±1 for some elements; therefore, it is essential to consider the mean value to estimate the maximum value of stress in the ship structure. These absolute values are roughly in the order $|\mu_{Y_1}| > |\mu_{Y_2}| > |\mu_{Y_3}|$, which is due to the correlation between the wave-induced load and still-water load. In addition, the absolute value of the alt.-condition is larger than that of the homo.-condition because under the alternative loading, high stress is likely to occur even in the still-water condition.

Figure 6 shows histograms of the ratios of the mean zero-upcrossing period between Y_i-component T_{zY_i} $(:= 2\pi\sigma_{Y_i}/\sigma_{\dot{Y}_i})$ and incident wave T_{ez}. Here, it can be seen that T_{zY_i} takes a value close to T_{ez} and differs by 20% at most. Therefore,

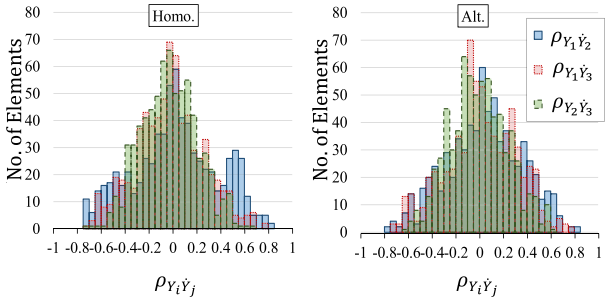

Fig. 8 Histograms of correlation coefficients between Y_i and $\dot{Y}_i$ for the 700 selected elements (left: homo., right: alt.)

considering that T_{ez} in $Q_Z(z)$ has a logarithmic effect on z, it can be approximated as $T_{ez} \cong T_{zY_i}$. Furthermore, we can say that $\sigma_{\dot{Y}_1}/\sigma_{Y_1} \cong \sigma_{\dot{Y}_2}/\sigma_{Y_2} \cong \sigma_{\dot{Y}_3}/\sigma_{Y_3}$. The reason why the period of the main component T_{zY_1} tends to be longer than T_{ez} is that the dominant load factor has a slightly longer period than the wave period in the MSS. This depends on the scale of the ship, and T_{zY_1} is expected to be shorter than T_{ez} for smaller ships.

Figures 7 and 8 show histograms of correlation coefficients between $\dot{Y}_i$ and $\dot{Y}_j (i \neq j)$ ($\rho_{\dot{Y}_i\dot{Y}_j} := \Sigma_{\dot{Y}_i\dot{Y}_j}/\sigma_{\dot{Y}_i}\sigma_{\dot{Y}_j}$) and between Y_i and $\dot{Y}_j (i \neq j)$ ($\rho_{Y_i\dot{Y}_j} := \Sigma_{Y_i\dot{Y}_j}/\sigma_{Y_i}\sigma_{\dot{Y}_j}$). It is found from Fig. 7 that the absolute value of $\rho_{\dot{Y}_i\dot{Y}_j}$ is at most 0.3; hence, Eq. (21) is a reasonable approximation. On the other hand, Fig. 8 shows that Eq. (20) does not hold because $\rho_{Y_i\dot{Y}_j}$ can be large. However, the effect of $\rho_{Y_i\dot{Y}_j}$ is secondary for the upcrossing rate [6] and thus Eq. (20) does not cause any problems, as will be confirmed numerically below.

4.3 Generation of time series for von Mises Stress

The extreme value distribution obtained from the generated time series of von Mises stress was also used for verification. The time series of $\mathbf{X}$ were generated from the RAOs of the stress components $\hat{X}_i$ and wave spectrum $\Phi_{\zeta\zeta}(\omega, \beta)$ with directional scatter, as follows.

$$x_i(t) = \sum_{n=1}^{N}\sum_{m=1}^{M} \left|\hat{X}_i(\omega_n, \beta_m)\right| \times \sqrt{2\Phi_{\zeta\zeta}(\omega_n, \beta_m)\Delta\omega_n\Delta\beta_m} \times \cos\left\{\omega_{en}t + \varepsilon_{n,m} + \varepsilon_{x_i}(\omega_n, \beta_m)\right\}, \quad (47)$$

$$\text{where } \omega_{en} := \omega_n - \frac{\omega_n^2}{g}U\cos(\beta_m), \quad (48)$$

and $\varepsilon_{n,m}$, the phase advance of the incident wave component, is a uniform random number in the range $[0, 2\pi]$. The time series of the von Mises stress was calculated from the time series of the stress components at each time step, and its extreme value distribution was obtained by picking up the maxima.

The ISSC wave spectrum was used for $\Phi_{\zeta\zeta}(\omega, \beta)$ [17]. Assuming an event in a short-term sea state, the duration of the time series and the number of repetitions are sufficiently large to numerically stabilize the extreme value distribution. Specifically, the spectrum was divided into 1000 equal areas against wave frequency ($N = 1000$) and into 5 parts against wave direction ($M = 5$). The duration of the time series was 2000 T_{ez} [s], and it was repeated 50 times with different random numbers of $\varepsilon_{n,m}$.

4.4 Comparison of extreme value distributions of von mises stress

We compared the proposed formula (46) for the extreme value distribution of Mises stress with the Madsen's exact formula (14) and the extreme value distribution obtained

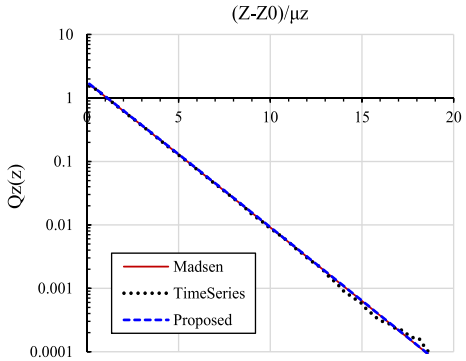

Fig. 9 Comparison of exceedance probabilities of peak value of Z at element A. $\sigma_{Y_2}/\sigma_{Y_1}$=0.23, $\sigma_{Y_3}/\sigma_{Y_1}$=0.004, $Z_0/\mu_Z = 0.072$

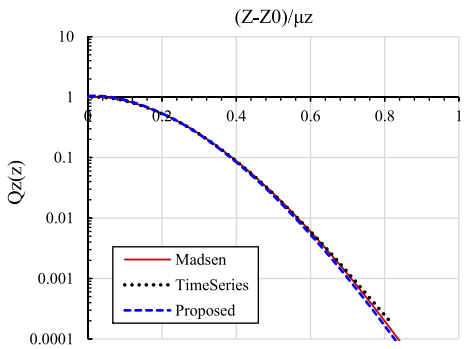

Fig. 10 Comparison of exceedance probabilities of peak value of Z at element B. $\sigma_{Y_2}/\sigma_{Y_1}$=0.78, $\sigma_{Y_3}/\sigma_{Y_1}$=0.24, $Z_0/\mu_Z = 0.98$

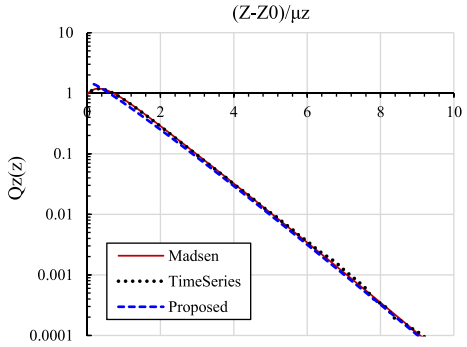

Fig. 11 Comparison of exceedance probabilities of peak value of Z at element C. $\sigma_{Y_2}/\sigma_{Y_1}$=0.65, $\sigma_{Y_3}/\sigma_{Y_1}$=0.33, $Z_0/\mu_Z = 0.41$

from the time series. First, we focused on the following three structural elements that have characteristic distributions.

(A) Typical element where the mean value and std. dev. ratio are small,
(B) Element where the still-water component Z_0 is large relative to the variable component, and
(C) Element where the std. dev. ratio $\sigma_{Y_2}/\sigma_{Y_1}$ is large.

The plot of the extreme value distribution $Q_Z(z)$ for each method is shown in Figs. 9, Fig. 10, and 11 for elements A, B, and C, respectively. The range of the horizontal axis is limited to $Z \geq Z_0$, because Z does not have to be estimated in the region smaller than Z_0 for practical use, and the upcrossing rate $\nu_Z^+(z)$ peaks near $Z = Z_0$ and is different from the actual distribution of $Q_Z(z)$ in $Z < Z_0$. From these figures, it can be seen that the proposed formula (46) is in good agreement with the Madsen's formula and the results of the time series. The wobble in the time series distribution for $Q < 1/1000$ is due to statistical instability. The shape of the distribution of element B differs from those of elements A and C. This can be understood from the following rough estimation formula obtained by Eq. (32):

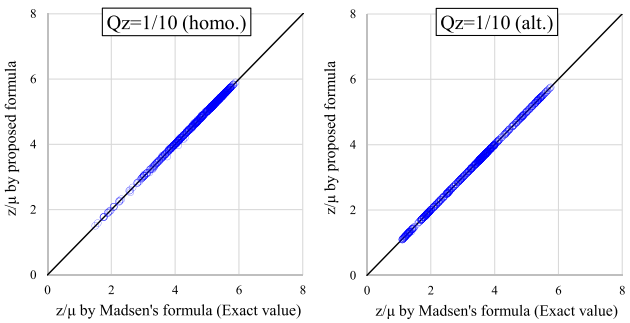

Fig. 12 Comparison of z levels of 700 selected elements when $Q_Z(z) = 1/10$ (left: homo., right: alt.)

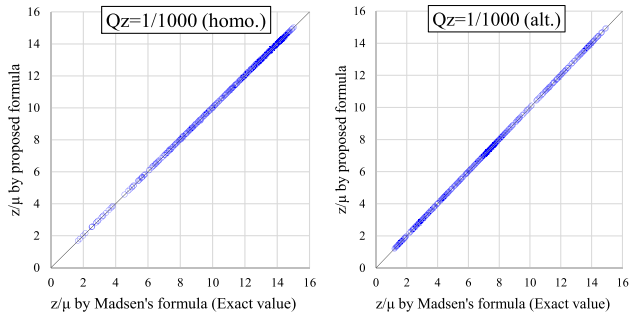

Fig. 13 Comparison of z levels of 700 selected elements when $Q_Z(z) = 1/1000$ (left: homo., right: alt.)

$$z(Q_Z) - Z_0 \cong -2\sigma_{Y_1}^2 \ln(Q_Z) + \mu_{Y_1}\sigma_{Y_1}\sqrt{-2\ln(Q_Z)}. \quad (49)$$

According to this equation, $Q_Z(z - Z_0)$ is close to being the square of the Rayleigh distribution ($\cong \exp[-(z - Z_0)/2\sigma_{Y_1}^2]$) when $Z_0/\mu_Z \to 0$, whereas it is close to a Rayleigh distribution ($\cong \exp[-(z - Z_0)^2/2\mu_{Y_1}^2\sigma_{Y_1}^2]$) when $Z_0/\mu_Z \to 1$.

Next, Figs. 12 and 13 compare Madsen's formula and the proposed formula for the level z at which $Q_Z(z) = 1/10$ and $1/1000$ for the two conditions and 700 selected elements. Since the distribution of extremes in the time series showed variations due to randomness, the results are compared with those of Madsen's formula (14), which is completely specified by the response spectrum. From these figures, it can be seen that the proposed formula (46) has very high accuracy. The small error at $Q_Z(z) = 1/10$ was mainly caused by the asymptotic expansion, while the approximation by Eqs. (20) and (21) had extremely small error. In other words, there is negligible difference between the Madsen's formula (14) and the integral on the plane-P in Eq. (22).

4.5 Applicable range of proposed formula

Finally, we investigated the applicable parameter range of the proposed formula (46). Here, we investigated the error distribution of the proposed formula in a five-parameter space: standard deviation ratios $\sigma_{Y_2}/\sigma_{Y_1}$, $\sigma_{Y_3}/\sigma_{Y_1}$ and mean values μ_{Y_1}, μ_{Y_2}, and μ_{Y_3}. The error rate γ is defined as

$$\gamma := \left(z_{Q=1/1000}^{\text{Formula}} - z_{Q=1/1000}^{\text{Exact}}\right)/z_{Q=1/1000}^{\text{Exact}}, \quad (50)$$

where $z_{Q=1/1000}^{\text{Formula}}$ is the value of z obtained from the proposed formula (46) that satisfies $Q_Z(z) = 1/1000$, and $z_{Q=1/1000}^{\text{Exact}}$ is the value obtained from Madsen's formula (14).

Figure 14 shows the contours of the error rate γ on the $\sigma_{Y_2}/\sigma_{Y_1}$-$\sigma_{Y_3}/\sigma_{Y_1}$ planes for six combinations, where μ_{Y_1}, μ_{Y_2}, and μ_{Y_3} are 0 or $3\sigma_{Y_1}$.The value of $3\sigma_{Y_1}$ was chosen because the error becomes relatively large. The upper limit of $\sigma_{Y_i}/\sigma_{Y_1}$

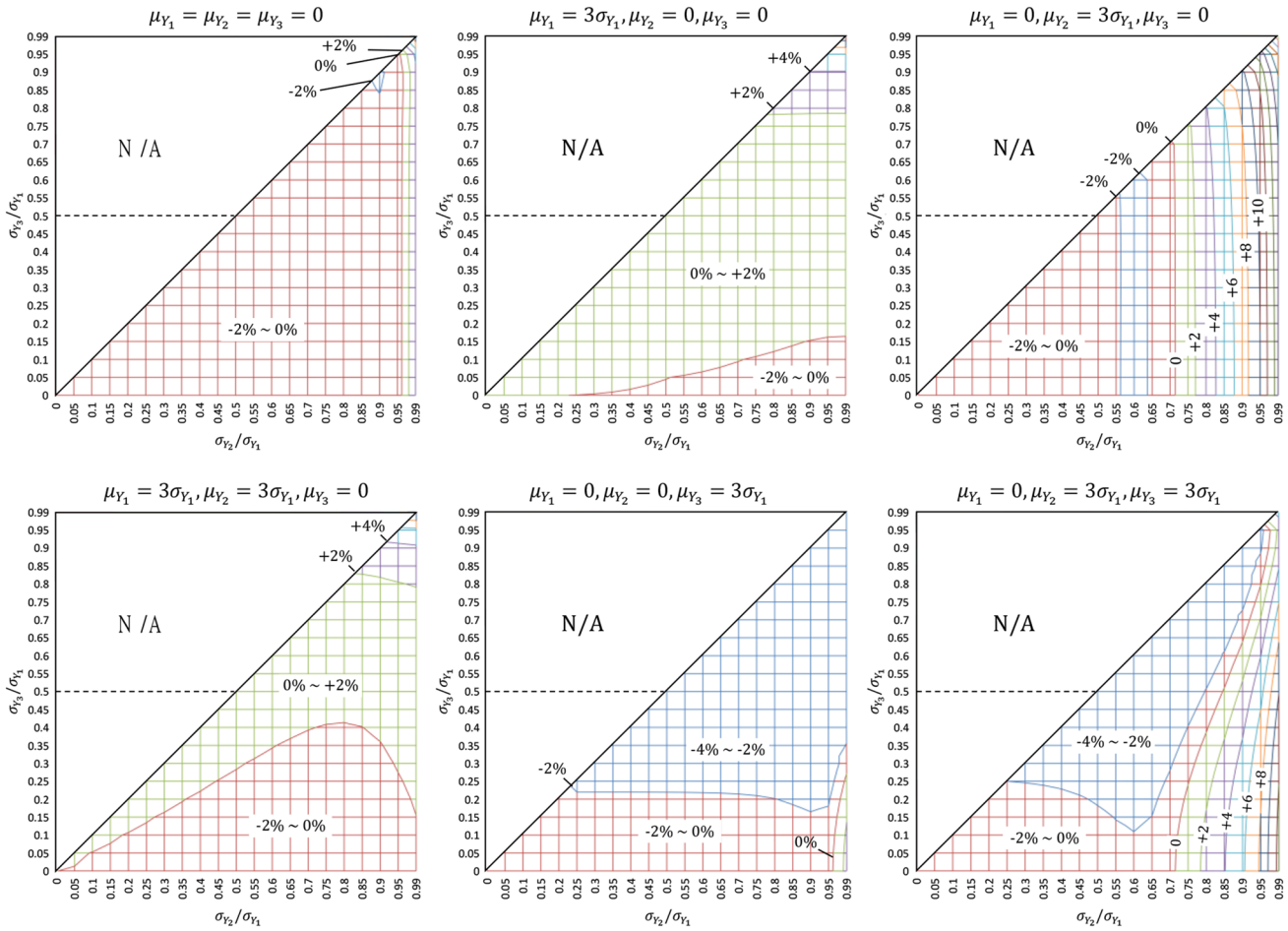

Fig. 14 Error rate distribution γ (%) of proposed formula in $\sigma_{Y_2}/\sigma_{Y_1}$-$\sigma_{Y_3}/\sigma_{Y_1}$ plane

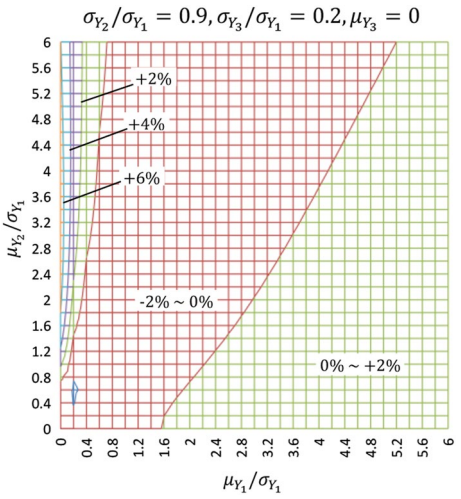

Fig. 15 Error rate distribution γ (%) of proposed formula in μ_{Y_1}/σ_{Y_1} -μ_{Y_2}/σ_{Y_1} plane

in Fig. 14 is set to 0.99 because the proposed formula goes to infinity as $\sigma_{Y_2}/\sigma_{Y_1} \to 1$, but this singularity does not cause a practical problem. Figure 15 shows the error rate γ on the μ_{Y_1}/σ_{Y_1}-μ_{Y_2}/σ_{Y_1} plane where $\sigma_{Y_2}/\sigma_{Y_1}=0.9, \sigma_{Y_3}/\sigma_{Y_1}=0.2$, and $\mu_{Y_3}=0$.

Figure 14 and 15 indicate that the accuracy of 2% is guaranteed for a wide range of parameters. However, in Fig. 14, when $\mu_{Y_1}=0$ and $\mu_{Y_2}=3\sigma_{Y_3}$ (upper right and lower right figures), the proposed formula over-estimates in the region $\sigma_{Y_2}/\sigma_{Y_1}>0.85$. This is because when $\left|\mu_{Y_2}/\mu_{Y_1}\right| \ll 1$, the distance between the two points $(y_1^{M\pm}, y_2^{M\pm})$, where ψ takes maximal value as shown in Fig. 2, becomes shorter, and these contributions overlap in the asymptotic Eq. (35). However, it is found from Fig. 15 that the region where γ has a large value is very close to the $\mu_{Y_1}=0$ axis and it is extremely rare for both $\mu_{Y_1} \cong 0$ and $\sigma_{Y_2}/\sigma_{Y_1}>0.85$ to be true (see Figs. 4 and 5). Therefore, although the proposed formula over-estimates by more than 5% under the condition

that $\left|\mu_{Y_2}/\mu_{Y_1}\right| < 0.02$ (from Fig. 15) and $\sigma_{Y_2}/\sigma_{Y_1} > 0.85$, there is little problem in practice.

5 Conclusion

The author proposed a practical method for estimating the extreme value distribution of von Mises stress that can be easily applied to ship design. The proposed method combines the variable transformation of stress components presented by Segalman and an asymptotic approximation for the integral of the upcrossing rate. The features of the proposed method are enumerated as follows.

(i) A closed formula for the upcrossing rate is given by making an asymptotic approximation of the integral in the case of stress components with non-zero mean value. The formula is based on an idea like that of Laplace's method, which is extended to the non-zero mean value case and the solution of the quartic equation of the reference point is simplified for an asymptotic expansion. Other approximations within realistic parameter ranges are applied; e.g., the transformed vector process and its time derivative are mutually independent and the standard deviation ratio between the variables is not large.

(ii) The computational procedure of the proposed method does not differ much from the conventional linear short/long-term statistical prediction. The only additional calculations are for deriving the covariance matrix of the stress components from the RAOs and wave spectrum and diagonalizing the 3×3 covariance matrix. The proposed method does not require the numerical integration commonly required by other methods; thus, robust results can be obtained at a low computational cost.

(iii) Through the structural analysis of a whole structural model of a bulk carrier in waves, it was confirmed that the proposed method has sufficient accuracy for the maximum expected value of von Mises stress. Furthermore, the parametric study clarified the application range of the proposed method and confirmed that the accuracy would not deteriorate for structures in waves.

6 Appendix 1. Variable Transformation of von Mises stress into Some of Squares Form

This appendix describes the procedure to obtain the covariance matrixes $\mathbf{\Sigma_{XX}}$, $\mathbf{\Sigma_{\dot{X}\dot{X}}}$, and $\mathbf{\Sigma_{X\dot{X}}}$ from the RAOs of $\mathbf{X}$ and the wave spectrum of short-crested irregular waves. Using these matrices, $\mathbf{X}$ is transformed into another vector process $\mathbf{Y}$ in which Z is expressed as a sum of squares.

Calculation of covariance matrix of X Let us denote the RAO of X_i as $\widehat{X}_i(\omega, \beta)$ (complex number), where ω and β are wave frequency and wave angle, respectively, and denote the wave spectrum of short-crested irregular waves as $\Phi_{\zeta\zeta}(\omega, \beta)$. The components of the covariance matrix $\mathbf{\Sigma_{XX}}$ in the short-term sea state can be calculated as

$$\begin{aligned}\Sigma_{X_iX_j} &= \int_{-\pi}^{\pi}\int_0^{\infty} \Phi_{\zeta\zeta} Re\left[\hat{X}_i\hat{X}_j^*\right] \mathrm{d}\omega\mathrm{d}\beta \\ &= \int_{-\pi}^{\pi}\int_0^{\infty} \Phi_{\zeta\zeta}\left|\hat{X}_i\right|\left|\hat{X}_j\right|\cos\left(\varepsilon_{X_i}-\varepsilon_{X_j}\right)\mathrm{d}\omega\mathrm{d}\beta,\end{aligned} \tag{51}$$

where the superscript "*" denotes the complex conjugate, ε_{X_i} is the phase advance of $\widehat{X}_i$ $(= \arg\left[\widehat{X}_i\right])$. Similarly, $\mathbf{\Sigma_{\dot{X}\dot{X}}}$ and $\mathbf{\Sigma_{X\dot{X}}}$ can be derived by replacing $\widehat{X} \to i\omega_e\widehat{X}$ in Eq. (51). The above equation defines the wave angle β such that $\beta = 0$ is a following sea and $\beta = \pi$ is a head sea. Thus, $\mathbf{\Sigma_{\dot{X}\dot{X}}}$ and $\mathbf{\Sigma_{X\dot{X}}}$ are calculated as

$$\Sigma_{\dot{X}_i\dot{X}_j} = \int_{-\pi}^{\pi}\int_0^{\infty} \omega_e^2\Phi_{\zeta\zeta}\left|\hat{X}_i\right|\left|\hat{X}_j\right|\cos\left(\varepsilon_{X_i}-\varepsilon_{X_j}\right)\mathrm{d}\omega\mathrm{d}\beta, \tag{52}$$

$$\begin{aligned}\Sigma_{X_i\dot{X}_j} = &\int_{-\pi}^{\pi}\int_0^{\infty} \omega_e\Phi_{\zeta\zeta}\left|\hat{X}_i\right|\left|\hat{X}_j\right| \\ &\times\cos\left(\varepsilon_{X_i}-\varepsilon_{X_j}-\frac{\pi}{2}\right)\mathrm{d}\omega\mathrm{d}\beta.\end{aligned} \tag{53}$$

Sum of squares expression of von Mises stress The procedure of standard normalization of the joint PDF of vector process $\mathbf{X}$ is commonly applied, but in addition, it is also possible to make its derivatives $\dot{\mathbf{X}}$ independent by orthogonal transformation. That is, without loss of generality, vector process $\mathbf{X}$ can be transformed into another vector process $\mathbf{V}$ which satisfies $\mathbf{\Sigma_{VV}} = \mathbf{I}$ and $\mathbf{\Sigma_{\dot{V}\dot{V}}} = \mathrm{diag}(\sigma^2_{\dot{V}_1}, \sigma^2_{\dot{V}_2}, \sigma^2_{\dot{V}_3})$, or $\mathbf{\Sigma_{\dot{V}\dot{V}}} = \mathbf{I}$ and $\mathbf{\Sigma_{VV}} = \mathrm{diag}(\sigma^2_{V_1}, \sigma^2_{V_2}, \sigma^2_{V_3})$ as can be seen in, e.g., Ref. [2, 6, 7]. However, in this study, we follow Segalman's method [8, 9], which standardizes the iso-ellipsoid of Z instead of the PDF of $\dot{\mathbf{X}}$. The procedure presented in this study is a modification of Segalman's method in which only one diagonalization is required.

First, we transform $\mathbf{X}$ so that the iso-ellipsoid of Z in $\mathbf{X}$ -space becomes a sphere, as follows.

$$\boldsymbol{\xi} = \mathbf{B}^{\mathrm{T}}\mathbf{X}, \tag{54}$$

where

$$\mathbf{B} := \mathbf{Q}\left(\boldsymbol{\lambda}^{\mathbf{A}}\right)^{1/2} = \begin{bmatrix} 1/2 & -\sqrt{3}/2 & 0 \\ 1/2 & \sqrt{3}/2 & 0 \\ 0 & 0 & \sqrt{3} \end{bmatrix}. \tag{55}$$

$\mathbf{Q}$ is an orthogonal matrix which diagonalizes $\mathbf{A}$, and $\boldsymbol{\lambda}^{\mathbf{A}}$ is a diagonal matrix ($= \mathrm{diag}\left(\lambda_1^A, \lambda_2^A, \lambda_3^A\right)$) where λ_i^A are the eigenvalues of $\mathbf{A}$, i.e., $\boldsymbol{\lambda}^{\mathbf{A}} = \mathbf{Q}^{\mathrm{T}}\mathbf{A}\mathbf{Q}$. Since Z in Eq. (2) can be expressed by a vector process $\boldsymbol{\xi}$,

$$Z = \boldsymbol{\xi}^{\mathrm{T}}\left\{\left(\boldsymbol{\lambda}^{\mathbf{A}}\right)^{-1/2}\mathbf{Q}^{\mathrm{T}}\mathbf{A}\mathbf{Q}\left(\boldsymbol{\lambda}^{\mathbf{A}}\right)^{-1/2}\right\}\boldsymbol{\xi} = \boldsymbol{\xi}^{\mathrm{T}}\boldsymbol{\xi} = \sum_{i=1}^{3}\xi_i^2, \quad (56)$$

the isosurface of Z is a sphere in $\boldsymbol{\xi}$-space. The covariance matrix of $\boldsymbol{\xi}$ can be obtained from

$$\boldsymbol{\Sigma}_{\boldsymbol{\xi}\boldsymbol{\xi}} = \mathbf{B}^{\mathrm{T}}\boldsymbol{\Sigma}_{\mathbf{X}\mathbf{X}}\mathbf{B}, \quad (57)$$

as can be understood from the transformation of the exponent portion of the joint PDF of $\mathbf{X}$, Eq. (1).

Next, we transform $\boldsymbol{\xi}$ into a vector process $\mathbf{Y}$ whose components are mutually independent by performing an orthogonal transformation. To do so, the diagonalization was conducted using an orthogonal matrix $\mathbf{R}$ as follows.

$$\boldsymbol{\Sigma}_{\mathbf{Y}\mathbf{Y}} = \mathbf{R}^{\mathrm{T}}\boldsymbol{\Sigma}_{\boldsymbol{\xi}\boldsymbol{\xi}}\mathbf{R} = \mathrm{diag}\left(\sigma_{Y_1}^2, \sigma_{Y_2}^2, \sigma_{Y_3}^2\right). \quad (58)$$

Here, the order is $\sigma_{Y_1} \geq \sigma_{Y_2} \geq \sigma_{Y_3}$. $\mathbf{Y}$ can be obtained by transforming as follows.

$$\mathbf{Y} = \mathbf{R}^{\mathrm{T}}\boldsymbol{\xi} = \mathbf{R}^{\mathrm{T}}\mathbf{B}^{\mathrm{T}}\mathbf{X}. \quad (59)$$

The vector process $\mathbf{Y}$ follows $\mathbf{Y} \sim \mathcal{N}\left(\boldsymbol{\mu}_{\mathbf{Y}}, \boldsymbol{\Sigma}_{\mathbf{Y}\mathbf{Y}}\right)$, where $\boldsymbol{\mu}_{\mathbf{Y}} = \mathbf{R}^{\mathrm{T}}\mathbf{B}^{\mathrm{T}}\boldsymbol{\mu}_{\mathbf{X}}$ and $\boldsymbol{\Sigma}_{\mathbf{Y}\mathbf{Y}}$ is a diagonal matrix as shown in Eq. (58). Furthermore, Z is expressed as a sum of squares of Y_i:

$$Z = \boldsymbol{\xi}^{\mathrm{T}}\boldsymbol{\xi} = \mathbf{Y}^{\mathrm{T}}\left(\mathbf{R}^{\mathrm{T}}\mathbf{R}\right)\mathbf{Y} = \sum_{i=1}^{3}Y_i^2. \quad (60)$$

The covariance matrix of $\dot{\mathbf{Y}}$, that is $\boldsymbol{\Sigma}_{\dot{\mathbf{Y}}\dot{\mathbf{Y}}}$, can also be derived by transforming $\boldsymbol{\Sigma}_{\dot{\mathbf{X}}\dot{\mathbf{X}}}$ as

$$\boldsymbol{\Sigma}_{\dot{\mathbf{Y}}\dot{\mathbf{Y}}} = \mathbf{R}^{\mathrm{T}}\mathbf{B}^{\mathrm{T}}\boldsymbol{\Sigma}_{\dot{\mathbf{X}}\dot{\mathbf{X}}}\mathbf{B}\mathbf{R}. \quad (61)$$

The same transform is applicable to $\boldsymbol{\Sigma}_{\mathbf{Y}\dot{\mathbf{Y}}}$ and $\boldsymbol{\Sigma}_{\dot{\mathbf{Y}}\mathbf{Y}}$.

Furthermore, the mean value of Z is expressed as the standard deviation and mean value of $\mathbf{Y}$, i.e.,

$$\begin{aligned}\mu_Z &= E\left[\sum_{i=1}^{3}Y_i^2\right] \\ &= \int_{-\infty}^{\infty}\int_{-\infty}^{\infty}\int_{-\infty}^{\infty}\sum_{i=1}^{3}y_i^2 f_{\mathbf{Y}}(\mathbf{y})\mathrm{d}y_1\mathrm{d}y_2\mathrm{d}y_3 \\ &= \sum_{i=1}^{3}\int_{-\infty}^{\infty}y_i^2 f_{Y_i}(y_i)\mathrm{d}y_i = \sum_{i=1}^{3}\left(\mu_{Y_i}^2 + \sigma_{Y_i}^2\right).\end{aligned} \quad (62)$$

Thus, it turns out that a nonlinear quantity Z expressed in any quadratic form can be expressed as a sum of squares of mutually independent Gaussian vector process $\mathbf{Y}$ which is obtained by making a linear transformation of $\mathbf{X}$. A schematic diagram of the above derivation process for the two-dimensional case is shown in Fig. 16. Here, it can be understood that this method is applicable when the isosurface of Z is an ellipsoid, i.e., that Z is in quadratic form.

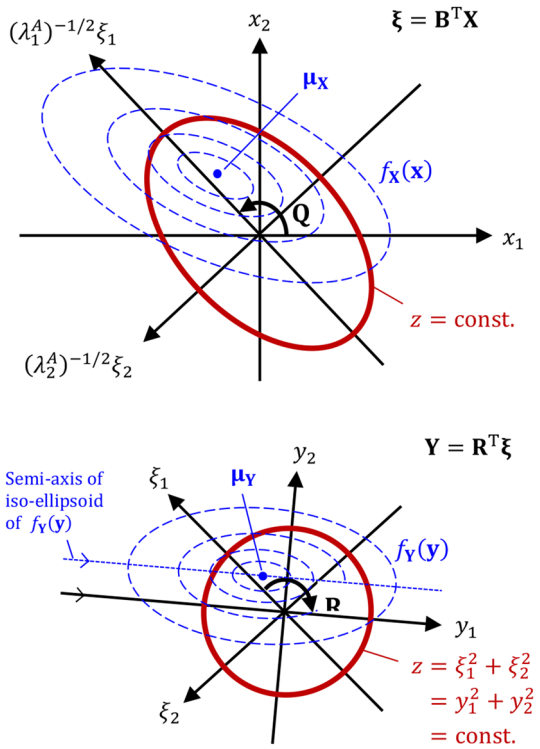

Fig. 16 Schema of the derivation of the standard deviation of the quadratic form in the case of 2-dimension

7 Appendix 2. Asymptotic expansion by Laplace's method

General case Let us consider the bi-variable Laplace integral,

$$I(z) = \int_a^b\int_c^d f(\theta,\phi)\exp\left[g(z,\theta,\phi)\right]\mathrm{d}\theta\mathrm{d}\phi, \quad (63)$$

where $f(\theta,\phi)$ and $g(z,\theta,\phi)$ are continuous real functions and $g(z,\theta,\phi)$ is an increasing function with respect to z. When $g(z,\theta,\phi)$ takes a maximum value at a point $(\theta,\phi) = \left(\theta_0,\phi_0\right)$ in the integration range, it can be asymptotically expanded using Laplace's method [14]. In this case, when z is sufficiently large, the integrand is dominated by the contribution near $(\theta,\phi) = \left(\theta_0,\phi_0\right)$. Therefore, substituting the Taylor expansion of $g(z,\theta,\phi)$ around $(\theta,\phi) = \left(\theta_0,\phi_0\right)$,

$$g(z,\theta,\phi) = g(z,\theta_0,\phi_0) + \frac{\theta^2}{2}g_{\theta\theta}(z,\theta_0,\phi_0) + \frac{\phi^2}{2}g_{\phi\phi}(z,\theta_0,\phi_0), \tag{64}$$

into the original integral (B.1), $I(z)$ asymptotes as follows.

$$I(z) \sim f(\theta_0,\phi_0)\exp\left[g(z,\theta_0,\phi_0)\right] \times \int_a^b \exp\left[\frac{\theta^2}{2}g_{\theta\theta}(z,\theta_0,\phi_0)\right]\mathrm{d}\theta \times \int_c^d \exp\left[\frac{\phi^2}{2}g_{\phi\phi}(z,\theta_0,\phi_0)\right]\mathrm{d}\phi \quad \text{as } z\to\infty. \tag{65}$$

Since the ranges of integration with respect to θ and ϕ are allowed to expand to $[-\infty,\infty]$, respectively, the following asymptotic expansion formula can be obtained by applying the Gaussian integral formula:

$$I(z) \sim \frac{2\pi}{\sqrt{g_{\theta\theta}(z,\theta_0,\phi_0)g_{\phi\phi}(z,\theta_0,\phi_0)}} \times f(\theta_0,\phi_0)\exp\left[g(z,\theta_0,\phi_0)\right] \quad \text{as } z\to\infty. \tag{66}$$

Zero-mean case Now, let us consider the case $\mu_{Y_i} = 0$ in the upcrossing rate formula (22), and let $f(\theta,\phi)$ and $g(z,\theta,\phi)$ be as follows.

$$f(\theta,\phi) = (2\pi)^{-2} z\sin\theta \times\sqrt{\sigma_{\dot{Y}_1}^2\sin^2\theta\cos^2\phi + \sigma_{\dot{Y}_2}^2\sin^2\theta\sin^2\phi + \sigma_{\dot{Y}_3}^2\cos^2\theta}, \tag{67}$$

$$g(z,\theta,\phi) = -\frac{z}{2}\left(\frac{\sin^2\theta\cos^2\phi}{\sigma_{Y_1}^2} + \frac{\sin^2\theta\sin^2\phi}{\sigma_{Y_2}^2} + \frac{\cos^2\theta}{\sigma_{Y_3}^2}\right). \tag{68}$$

When $\sigma_{Y_1} > \sigma_{Y_2}, \sigma_{Y_3}$, $g(\theta,\phi)$ takes the maximum value at $\theta_0 = \pi/2$ and $\phi_0 = 0$. Accordingly, the following equations are derived.

$$f(\theta_0,\phi_0) = (2\pi)^{-2} z\sigma_{\dot{Y}_1}, \tag{69}$$

$$g(z,\theta_0,\phi_0) = -\frac{z}{2\sigma_{Y_1}^2}, \tag{70}$$

$$g_{\theta\theta}(z,\theta_0,\phi_0) = z\left(\frac{1}{\sigma_{Y_1}^2} - \frac{1}{\sigma_{Y_3}^2}\right), \tag{71}$$

$$g_{\phi\phi}(z,\theta_0,\phi_0) = z\left(\frac{1}{\sigma_{Y_1}^2} - \frac{1}{\sigma_{Y_2}^2}\right). \tag{72}$$

Substituting these into Eq. (66), we obtain the following equation.

$$I(z) \sim \frac{\sigma_{\dot{Y}_1}}{2\pi\sqrt{\left(\frac{1}{\sigma_{Y_1}^2} - \frac{1}{\sigma_{Y_2}^2}\right)\left(\frac{1}{\sigma_{Y_1}^2} - \frac{1}{\sigma_{Y_3}^2}\right)}}\exp\left[-\frac{z}{2\sigma_{Y_1}^2}\right] \quad \text{when } \mu_{Y_1} = \mu_{Y_2} = \mu_{Y_3} = 0, \text{ as } z\to\infty. \tag{73}$$

Considering that $g(\theta,\phi)$ takes a maximum at two points $\phi_0 = 0, \pi$ and the integrands at them have the same value, $I(z)$ must be doubled, i.e., $v_Z^+(z) = 2I(z)$. Thus, the asymptotic formula for the upcrossing rate, Eq. (33), is obtained.

8 Appendix 3. Derivation of Eq. (41)

Let us consider an explicit expression of (x, y) which satisfies the relationships of Eqs. (38) and (40). Here, we assume that μ_{Y_1} is positive and consider y_2^P in the region $y_1^P > 0$.

Equation (40) is transformed as follows.

$$y_2^P = c_{21}\mu_{Y_2} + \frac{c_{12}c_{21}\mu_{Y_1}\mu_{Y_2}}{y_1^P - c_{12}\mu_{Y_1}}. \tag{74}$$

From this expression, it is found that $y_2^P(\zeta)$ asymptotes as follows when ζ is sufficiently large.

$$y_2^P \sim c_{21}\mu_{Y_2} + \frac{c_{12}c_{21}\mu_{Y_1}\mu_{Y_2}}{\zeta} + O\left(\frac{1}{\zeta^2}\right) \text{ as } \zeta\to\infty. \tag{75}$$

Here, as a function $y_2^P(\zeta)$ which satisfies Eq. (75) and $y_2^P(0) = 0$, the following expression can be considered

$$y_2^P = \frac{c_{21}\mu_{Y_2}}{1 - c_{12}\mu_{Y_1}/\zeta}. \tag{76}$$

However, considering that Eq. (38), y_2^P must satisfy $y_2^P \le \zeta$, whereas Eq. (76) can be larger than ζ when ζ is small. Hence, we apply shear mapping to the curve of Eq. (76) in the y_2^P-ζ plane so that $y_2^P \le \zeta$ holds in $\zeta^2 \ge \mu_{Y_1}^2 + \mu_{Y_2}^2$ and maintains the properties of Eq. (C.2); i.e., by transforming $\zeta \to \zeta - \alpha y_2^P/\mu_{Y_2}$, Eq. (76) becomes

$$y_2^P = \frac{c_{21}\mu_{Y_2}}{1 - c_{12}\mu_{Y_1}/\{\zeta - (\alpha y_2^P/\mu_{Y_2})\}}, \tag{77}$$

where the real coefficient α is determined to pass through the point $(y_1^P, y_2^P) = (\mu_{Y_1}, \mu_{Y_2})$. Equation (41) is obtained by solving Eq. (77) for y_2^P. Subsequently, by substituting $(y_1^P, y_2^P) = (\mu_{Y_1}, \mu_{Y_2})$ into Eq. (77), α is determined to be as in Eq. (42).

Acknowledgements The author would like to thank Dr. Toichi Fukasawa of the National Maritime Research Institute, Japan for his advice

and careful proofreading of this manuscript. The author is also grateful to Mr. Kei Sugimoto at ClassNK for useful discussions.

References

1. Fukuda J-i (1969) Statistical prediction of ship response. In: Symposium on seakeeping, The Society of Naval Architects of Japan, pp. 99–119 (**in Japanese**)
2. Veneziano D, Cornell CA, Grigoriu M (1977) Vector-process models for system reliability. J Eng Mech-Asce 103:441–460
3. Madsen H (1985) Extreme-value statistics for nonlinear stress combination. J Eng Mech 111:1121–1129
4. Gupta S, Manohar C (2005) Probability distribution of extremes of von mises stress in randomly vibrating structures. J Vib Acoust 127:547–555
5. Breitung K (1988) Asymptotic crossing rates for stationary Gaussian vector processes. Stoch Process Appl 29(2):195–207
6. Hagen Ø (1993) Outcrossing of stationary Gaussian process from 2D elliptical region. J Eng Mech-Asce 119:973–996
7. Leira BJ (1994) Multivariate distributions of maxima and extremes for Gaussian vector-processes. Struct Saf 14(4):247–265
8. Segalman D, Reese G, Field R (2013) Probability Distribution of von Mises Stress in the Presence of Pre-Load, Sandia Report, SAND2013–3429
9. Segalman D, Reese G, Field Jr. R, Fulcher C (1999) Estimating the Probability Distribution of von Mises Stress for Structures Undergoing Random Excitation Part 1: Derivation. J Vib Acoust 122(1):42–48
10. Rice SO (1944) Mathematical analysis of random noise. Bell Syst Tech J 23(3):282–332
11. Fukuda J-I, Shinkai A, Tsukuda H (1980) On the statistical distribution of the maxima of non-linear stress induced on the ship hull in sea waves. J Soc Naval Arch Jpn 148:138–147 (**in Japanese**)
12. Leira B (2003) Extremes of Gaussian and non-Gaussian vector processes: a geometric approach. Struct Saf 25:401–422
13. Segalman D, Reese G, Field R (2018) Probability distribution of von mises stress in the presence of pre-load. Spec Top Struct Dyn 5:165–179
14. Small, C. G. (2010) Expansions and asymptotics for statistics. Chapman and Hall/CRC
15. Matsui S, Murakami C, Hayashibara H, Fueki R (2019) Development of direct load and structure analysis and evaluation system on whole ship DLSA-basic for ship structural design. Papers Natl Mari Res Inst 19:1–21 (**in Japanese**)
16. Kawabe H, Morikawa M, Shibazaki K (2001) Simple estimation method for long-term distribution of wave induced load based on the severest wave condition approach. J Soc Naval Arch Jpn 189:193–200 (**in Japanese**)
17. IACS (2001) No.34 Standard Wave Data